Application of Simulated Annealing and Genetic Algorithms to the Reconstruction of Electrical Permittivity Images in Capacitance Tomography

C Ortiz-Alemán, R Martin, J C Gamio and A Nicolas

Instituto Mexicano del Petróleo, Eje Central L Cárdenas 152, México, DF, 07730, México
jcortiz@imp.mx

ABSTRACT

In this work we apply the simulated annealing (SA) and genetic algorithms (GA) inversion methods to the reconstruction of permittivity images from electrical capacitance tomography (ECT) measurements. The forward problem (i.e., to find the mutual capacitance data for a given permittivity distribution in the sensor) is calculated by using a finite-volume space discretization method in order to avoid singularity problems at the centre of the pipe (as occurs with the finite difference method), and to take advantage from the conservative formulation of finite element methods. We test the GA and SA inversion methods using static physical models simulating the typical distribution patterns of two-component flow. The GA and SA-based permittivity inversions have some advantages over other approaches based on damped least-squares inversion: they can find good solutions starting with poor initial models, can more easily implement complex a priori information, and do not introduce smoothing effects in the final permittivity distribution model. A major disadvantage comes from the fact that GA and SA are computationally intensive and lead to relatively slow reconstructions.

Keywords Simulated annealing, Genetic algorithms, Capacitance tomography, Global optimisation, Finite volumes.

1 INTRODUCTION

Electrical capacitance tomography (ECT) is a technique for obtaining cross-sectional images of the electrical permittivity distribution inside an electrically non-conducting body or region (Xie, 1989; 1992). It can be used to map the composition of two-phase mixtures like gas-oil, and thus has important potential applications in the petroleum industry, for multiphase flow visualisation and measurement (Yang, 1995a; 1995b). In this context, an ECT sensor consists of an electrically insulating pipe with a number of electrodes on its outer wall, surrounded by an external screen (figure 1). The use of the cylindrical end guards permits the sensor to be modelled as a two-dimensional problem (Xie, 1989).

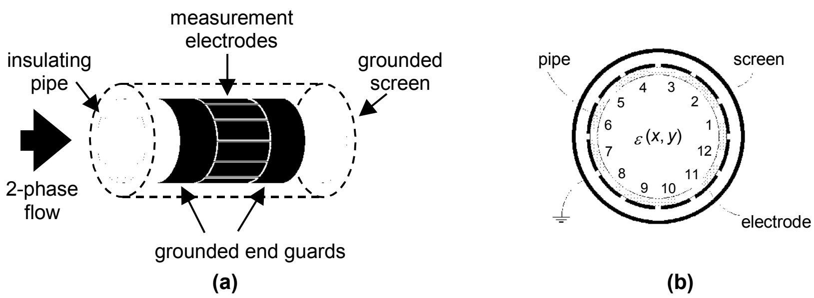

Figure 1: Electrical capacitance tomography sensor: (a) whole assembly and (b) cross-section

The sensor is connected to an apparatus that measures the mutual capacitance between all possible electrode pairs (figure 2). The measured data are fed into a computer where, by means of a suitable reconstruction algorithm, the data are inverted and an image of the permittivity distribution inside the sensor is produced. There are many alternative image reconstruction algorithms available (Isaksen, 1996; Yang, 2003), from fast but only qualitative linear back-projection (LBP), to quantitative but slower iterative least-squares optimisation schemes coupled with regularisation techniques. However, the reconstruction accuracy of these methods is still not quite good. They usually introduce unwanted smoothing in the reconstructed images (if the regularisation is too strong) or may become unstable and/or not converge to the desired solution (if the regularisation is too weak). The problems with linearized inversion schemes are fairly well known: they require that the starting model be close to the true solution as they typically attempt to find a local minimum in the close neighbourhood of the starting solution. They use local properties of the misfit function to calculate and update to the current model and search in the downhill direction. Problems which are not too labour intensive in forward modelling are better achieved by using global optimisation methods. These methods become more attractive than do local methods because they overcome many of the classical limitations. As mentioned above, local methods often depend strongly on the starting model, and are prone to entrapment in local minima. Moreover, they need the calculation of derivative information that can be difficult and costly (Gallagher, 1991).

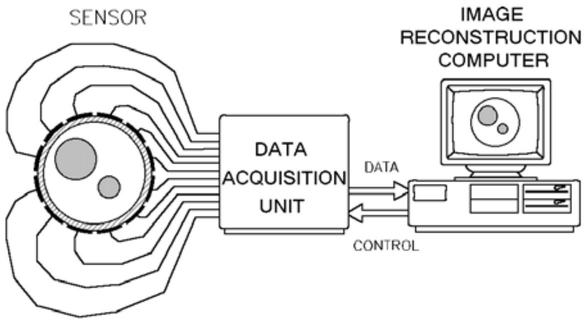

Figure 2: Electrical capacitance tomography (ECT) system

Inversion in this context involves finding an optimal value of a misfit function of several variables that describes the differences between measured and synthetic capacitance data by using an assumed permittivity model. Such a misfit surface as a function of model parameters is highly complicated and characterised by multiple hills and valleys. Global optimisation techniques, which include Monte Carlo, GA and SA methods, constitute alternative approaches to deal with this kind of highly non-linear optimisation problems. The issue has generated considerable interest in the field of artificial intelligence, and during the last decade in multi-parameter optimisation problems from other fields of technology (Rodriguez-Zuñiga, 1997). Both GA and SA were conceived from natural optimisation systems. GA uses an analogy with biological evolution and SA has an analogy with thermodynamics, specifically with the way that liquids freeze and crystallise, or metals cool and anneal. In this study we explore the applicability of GA and SA to the reconstruction of permittivity images from ECT measurements. These methods do not require a good starting model but are computationally more expensive. As pointed out by Yang (2003) in a recent review article on image reconstruction methods for ECT, currently most algorithms are based on simplified linear mathematical models. As ECT systems are essentially nonlinear, those authors recommend this kind of investigation on nonlinear techniques for both forward modelling and image reconstruction.

2 GENETIC ALGORITHMS AND SIMULATED ANNEALING

GA and SA can be identified as non-linear multiparameter optimisation methods. Both procedures are stochastic search techniques.

Pioneered by John Holland (1975), GA method has been referred as an evolution from Monte Carlo methods for strongly non-linear optimisation problems (Gallagher, 1991). GA is a powerful tool for locating an optimal model by rapidly exploring model space, it makes use of a stochastic search through model space employing a transition probability rule to improve the solution. Large and complex models are represented like binary coded strings. Mechanics of natural selection and genetics are applied to a randomly chosen initial population of models. Selection, crossover and mutation processes update the models, resulting in a new generation of “chromosomes”, emulating the way biological systems evolve to produce more successful organisms. The whole process is repeated until the mean of the fitness function is close to the maximum fitness of the population. The major procedure is summarised in the flow diagram of figure 3.

SA is also a generalization of Monte Carlo methods for examining the equations of state and frozen states of n-body systems (Metropolis, 1953). The concept is based on the way liquids freeze or metals recrystalize in the process of annealing. In this process, an initially high temperature melt is slowly cooled down allowing the system to stay in thermodynamic equilibrium. As the process continues the system becomes completely ordered and approaches to a frozen ground state.

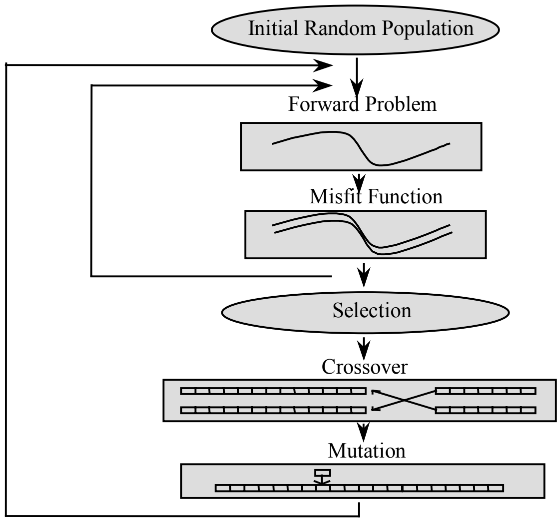

Figure 3: Basic steps of the GA based code

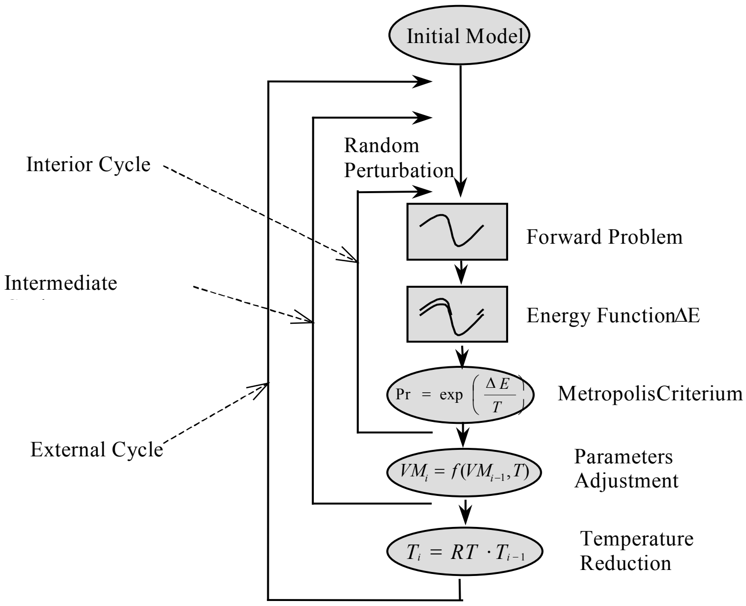

Figure 4: Basic steps of the SA based code

Generalization of this approach to optimisation problems is straight forward (Kirkpatrick, 1983): the current solution of the optimisation problem corresponds to the current state of the system, the objective function represents the energy function of the system, and the global minimum is analogous to the ground state. To make use of the Metropolis algorithm, we followed the general procedure depicted in the flow chart of figure 4. For a much more detailed description of both methods the reader is referred to Davis (1990).

3 FORWARD MODELLING

The forward problem is solved by using a finite volume method in a cylindrical configuration, in order to avoid undefined solutions at the disk centre and make the mesh refinement more flexible in comparison with finite element methods. We solved the following equations:

$$\nabla \cdot (\varepsilon \nabla \varphi) = 0, \tag{1}$$

where ε are given permittivities in the disk domain and φ is the potential field to be computed. Defining the radius and angle coordinates as r and θ, and using the finite volume method, the discretized equation is formulated in the conservative form on each cell Ω_{ij}:

$$\int_{\Omega_{ij}} \nabla \cdot (\varepsilon \nabla \varphi) \partial \Omega_{ij} = 0 \quad \text{for i=1,...,m and j=1,...,n} \tag{2}$$

Applying Gauss theorem, and using polar coordinates, the discretized equations can be written as:

$$\int_{\Gamma_{ij}} \varepsilon \nabla \varphi \partial \Gamma_{ij} = 0, \tag{3}$$

where Γ_{ij} is the boundary of the finite volume cell Ω_{ij}. The boundary Γ_{ij} is defined by Γ_W and Γ_E along the radial coordinates, and Γ_N and Γ_S along the angular coordinates. Equation (3) can be expressed as the sum of the fluxes across faces $\Gamma_{W,E,N,S}$:

$$\sum \int_{\Gamma_k} \varepsilon \nabla \varphi \cdot n_k \partial \Gamma_k = (\varepsilon / r)(\partial \varphi / \partial \theta)\Delta r\Big|_{i+1/2,j} - (\varepsilon / r)(\partial \varphi / \partial \theta)\Delta r\Big|_{i-1/2,j} + \varepsilon(\partial \varphi / \partial \theta) r \Delta \theta\Big|_{i,j+1/2} - \varepsilon(\partial \varphi / \partial \theta) r \Delta \theta\Big|_{i,j-1/2} \tag{4}$$

The capacitance on each electrode is computed integrating the potential gradients along the electrode length according to the following expression:

$$C_{ij} = -\varepsilon_0 / V_j \int_{\Gamma_i} \varepsilon \nabla \varphi \cdot n_i \partial \Gamma_i \tag{5}$$

where n_i is the normal to the electrode contour Γ_i, V_j is the potential of the sender electrode and ε_o is the vacuum permittivity.

4 RESULTS

In order to test the feasibility of GA and SA methods, we computed sets of ECT synthetic data for three typical permittivity distributions by means of our finite volume forward routine. Both algorithms were implemented in Fortran 90 on a Pentium IV PC with a 2.2 GHz CPU. We employed a 240 X 120 grid in the forward problem solution but results are valid for any larger dimensions. We simulated a twelve-electrode ECT sensor and capacitance values for all single-electrode combinations were calculated. We considered a two-component distribution with a lower permittivity material of 1.0 (air) and a higher permittivity material of 2.5 (oil). In the first two cases (annular and stratified flows), we restricted our numerical test to the reconstruction of noise free ECT data. In a third case (bubbly flow) we added a random noise level of 5% into the capacitance data.

After an appropriate parameterization, both methods produced very similar results for all three study cases. The quality of the reconstructed permittivity images mainly depends on the number of forward problem calculations. In figure 5, we present image reconstructions with the SA method (which are slightly better than GA reconstructions) for a simplified annular type flow after 30,000 and 60,000 forward problem computations. We present similar plots in figure 6 for a stratified flow.

In order to establish comparisons of results from both methods we stopped the process at 60,000 forward problem calculations for all three cases. We used the L_2 norm as objective or misfit function of theoretical results and data. CPU times are roughly the same (~25 minutes) for both GA and SA methods but memory allocation is much higher for the GA method because it requires the storage of a large binary coded matrix of models population. Convergence rates are better for GA in the beginning of the process but SA gets slightly better results at the end of the whole inversion process.

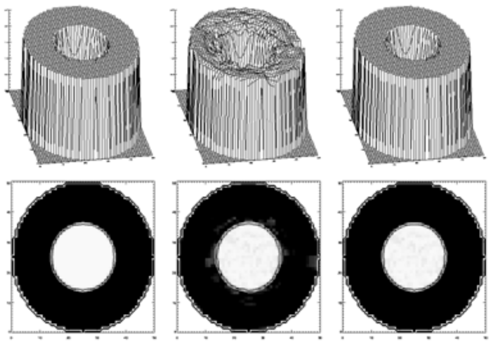

(a) (b) (c)

Figure 5: Annular flow image reconstructions: (a) test image (white value represents permittivity of air and black corresponds to oil permittivity); (b) reconstructed image after 30,000 forward problem computations; (c) image after 60,000 computations.

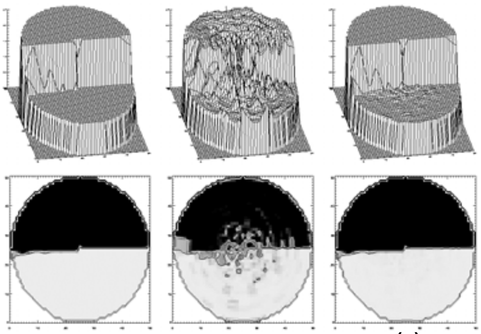

(a) (b (c)

Figure 6: Stratified flow image reconstructions: (a) test image (white value represents permittivity of air and black corresponds to oil permittivity); (b) reconstructed image after 30,000 forward problem computations; (c) image after 60,000 computations.

We considered a third case of noisy capacitance data for a permittivity distribution representing a simplified bubbly flow. In figure 7, we show a plot of the random noise vector (5% in relative magnitude) added to the capacitance signal (c) and a logarithmic plot of the true capacitances in farads ((d), in continuous line) and the noisy signal (over plotted with x symbols). In the log plot, true and noisy capacitances look pretty much the same as differences are linearized. Also in figure 7 we show the test distribution (a) and the reconstructed image (b) after 60,000 computations of the forward problem. The convergence rate is slightly lower than in the case of noise-free data for this level of noise.

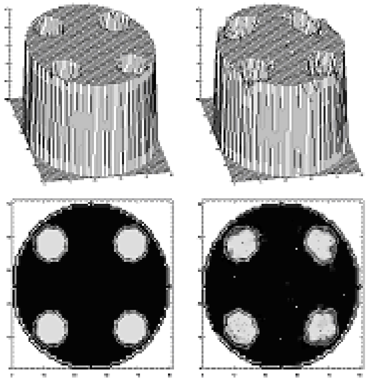

(a) (b)

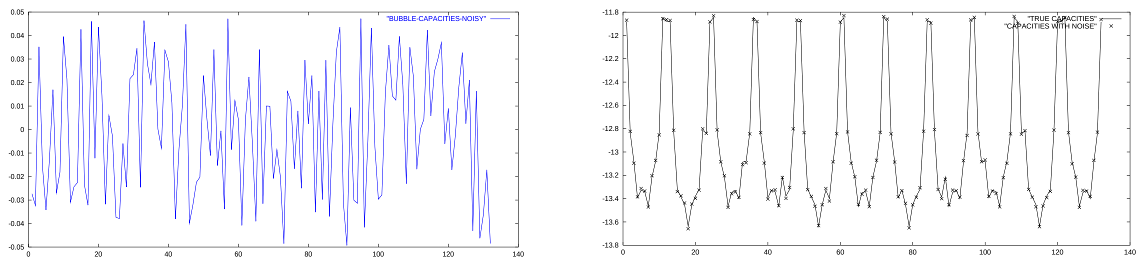

(c) (b)

Figure 7: Bubbly flow image reconstructions: (a) test image (white value represents permittivity of air and black corresponds to oil permittivity); (b) reconstructed image after 70,000 forward problem computations; (c) random noise vector added to the true capacitance signal for this simulation; (d) true (continuous line) and noisy (x symbols) capacitances inverted in this simulation. Note that we employed a Y logarithmic scale for this plot.

Application of GA and SA to the inversion of synthetic ECT data has provided us with very encouraging results even in the case of noise contaminated data. In this work we followed the advice of Yang and Peng (2003) to test nonlinear methods for both forward modelling (Finite Volume method) and reconstruction of electrical permittivity images by means of global inversion methods (GA and SA).

One criticism of both GA and SA methods is their relatively high computation time as they require several thousands of forward problem computations. Two interesting research matters, which we will explore in further work, are acceleration of these methods by the use of high performance parallel computing and combination of global optimisation with fast local search methods such as the linear back projection method.

5 REFERENCES

DAVIS L. (ed), (1990), Genetic Algorithms and Simulated Annealing, Pitman, London.

GALLAGHER K., SAMBRIDGE M. and DRIJKONINGEN G., (1991), Genetic algorithms: an evolution from Monte Carlo Methods for strongly non-linear geophysical optimization problems. *Geophys. Res. Lett.*, 18, 2177-2180.

HOLLAND J.H., (1975), Adaptation in Natural and Artificial Systems, University of Michigan Press.

ISAKSEN O., (1996), A review of reconstruction techniques for capacitance tomography, *Measurement Science and Technology*, vol. 7, pp 325–37.

METROPOLIS N., ROSENBLUETH A., ROSENBLUETH M., TELLER A. and TELLER E., (1953), Equation of state calculations by fast computing machines, J. *Chem. Phys.*, 21, 1087-1092.

RODRÍGUEZ-ZÚÑIGA J.L., ORTIZ-ALEMAN C., PADILLA G. and GAULON R., (1997), Application of genetic algorithms to constrain shallow elastic parameters using *in situ* ground inclination measurements, *Soil Dyn and Earth Eng*,, 16, 3, 223-234.

XIE C.G., PLASKOWSKI A. and BECK M.S., (1989), 8-electrode capacitance system for two-component flow identification. Part 1: Tomographic flow imaging, *IEE Proceedings A*, 136, pp 173-183.

XIE C.G., HUANG S.M., HOYLE B.S., THORN R., LENN C., SNOWDEN D. and BECK M.S., (1992), Electrical capacitance tomography for flow imaging: System model for development of image reconstruction algorithms and design of primary sensors, *IEE Proc.-G*, 139 (1), pp 89-98.

YANG W.Q., BECK M.S. and BYARS M., (1995a), Electrical capacitance tomography: from design to applications, *Measurement and Control*, 28, p 261.

YANG W.Q., STOTT A. L., BECK M. S. and XIE C. G., (1995b), Development of capacitance tomographic imaging systems for oil pipeline measurements, *Rev. of Scientific Instruments*, 66, 4326.

YANG W.Q. and PENG L., (2003), Image reconstruction algorithms for electrical capacitance tomography, *Measurement Science and Technology*, vol. 14, pp R1-R13.